Control of leaf morphogenesis by microRNAs

Javier F. Palatnik[1,2], Edwards Allen[3], Xuelin Wu[2]*, Carla Schommer[1]*, Rebecca Schwab[1]*, James C. Carrington[3] & Detlef Weigel[1,2]

[1]*Department of Molecular Biology, Max Planck Institute for Developmental Biology, D-72076 Tübingen, Germany*
[2]*Plant Biology Laboratory, The Salk Institute for Biological Studies, La Jolla, California 92037, USA*
[3]*Center for Gene Research and Biotechnology and Department of Botany and Plant Pathology, Oregon State University, Corvallis, Oregon 97331, USA*

* These authors contributed equally to this work

Plants with altered microRNA metabolism have pleiotropic developmental defects, but direct evidence for microRNAs regulating specific aspects of plant morphogenesis has been lacking. In a genetic screen, we identified the *JAW* locus, which produces a microRNA that can guide messenger RNA cleavage of several *TCP* genes controlling leaf development. MicroRNA-guided cleavage of *TCP4* mRNA is necessary to prevent aberrant activity of the *TCP4* gene expressed from its native promoter. In addition, overexpression of wild-type and microRNA-resistant *TCP* variants demonstrates that mRNA cleavage is largely sufficient to restrict *TCP* function to its normal domain of activity. *TCP* genes with microRNA target sequences are found in a wide range of species, indicating that microRNA-mediated control of leaf morphogenesis is conserved in plants with very different leaf forms.

Although much is known about how organs acquire their particular fate, we are only starting to learn how organs are sculpted, even if they are just flat sheets such as wings or leaves. An elegant study recently demonstrated that making a flat organ is not a trivial problem: snapdragon leaves are normally flat, but they become crinkly in plants lacking the *CINCINNATA (CIN)* gene[1]. In *cin* mutants, differential regulation of cell division across the leaf is disturbed, causing negative leaf curvature. *CIN* RNA itself is expressed in a dynamic pattern, in front of and perhaps overlapping the mitotic arrest zone, suggesting a direct role of *CIN* in regulating leaf morphogenesis.

Although it is unknown how expression of *CIN*, which encodes a TCP transcription factor[2], is regulated, a specific RNA pattern can result from differential transcription or changes in transcript stability. A post-transcriptional mechanism that has only recently been recognized is that of plant mRNA cleavage initiated by partially or fully complementary microRNAs (miRNAs)[3,4]. The mechanism of cleavage is similar, or identical, to cleavage guided by short interfering RNAs (siRNAs)[5].

The double-stranded ribonucleases Dicer in animals and DICER-LIKE1 (DCL1) in plants process miRNAs—which are usually 21–22 nucleotides long—from longer precursor RNAs with fold-back structure[4,6,7]. Additional factors required for accumulation of miRNAs include members of the Argonaute family and HEN1 protein[8,9]. The importance of miRNAs for plant development is supported by the abnormalities seen in several mutants or transgenic plants with general defects in miRNA accumulation or activity[9–12]. However, although biochemical studies have demon-

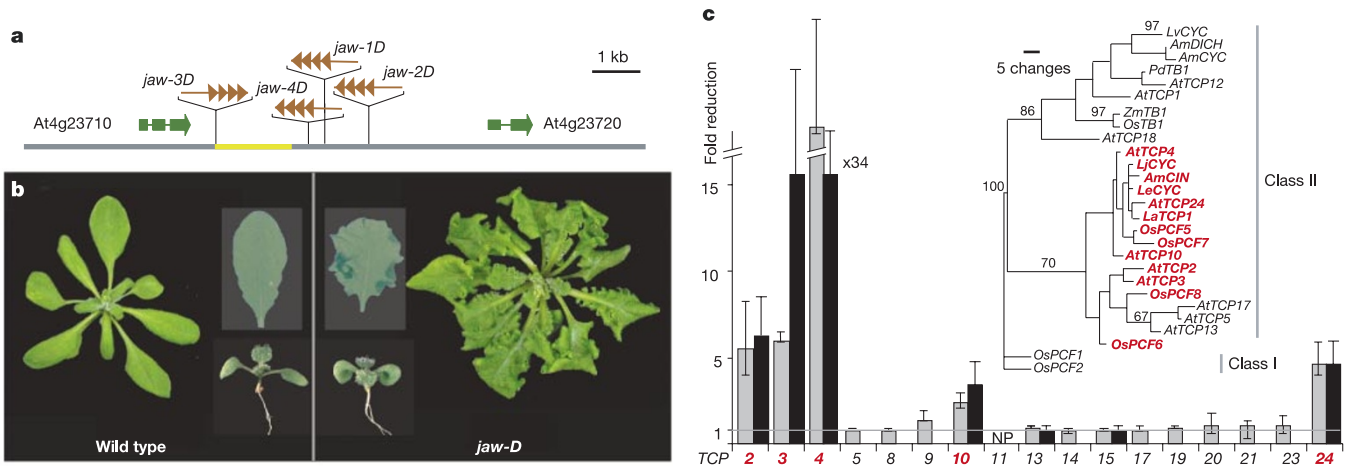

Figure 1 *jaw-D* mutations and effect of *jaw-D* on *TCP* genes. **a**, Insertion sites of *jaw-D* alleles relative to annotated genes. Triangles indicate *35S* enhancers on the T-DNA vectors. The yellow bar indicates the fragment used for recapitulation (see Fig. 2b). **b**, Seedlings, individual leaves and leaf rosettes of Columbia wild-type and *jaw-1D* plants. Leaves were mounted between glass plates and illuminated from below. Dark green areas indicate overlapping leaf parts after flattening. **c**, Expression changes of *TCP* genes in *jaw-1D* estimated from Affymetrix arrays (grey bars) or from RT–qPCR (black bars). See Supplementary Information for absolute values. NP, termed 'not present' by MAS software. Note that the Affymetrix probe sets hybridize to 3′ sequences shared by full-length and cleaved transcripts, whereas the RT–qPCR products span the miRNA-guided cleavage sites and are therefore specific for the full-length transcripts. Inset shows phylogenetic tree of TCP domains, with two class I proteins[2,38] as an out group. Red text indicates genes with miR-JAW target sequence. Am, *Antirrhinum majus* (snapdragon); At, *Arabidopsis thaliana*; La, *Lupinus albus*; Le, *Lycopersicon esculentum*; Lj, *Lotus japonicus*; Lv, *Linaria vulgaris*; Os, *Oryza sativa*; Pd, *Populus deltoides*; Zm, *Zea mays*.

strated that many plant miRNAs can guide cleavage of specific target mRNAs[3,4,13], the evidence for involvement of mRNA cleavage in specific biological processes has only been circumstantial.

Here, we describe an *Arabidopsis* miRNA, miR-JAW, with sequence complementarity to several *TCP* genes. MiR-JAW overexpression affects a subset of *TCP* genes, which represent the *Arabidopsis* homologues of *CIN*. The importance of miRNA-guided degradation is demonstrated with miRNA-resistant forms of target mRNAs that encode the same proteins as the wild-type genes.

Identification of the *JAW* locus and *JAW* target genes

The *JAW* locus is defined by four dominant alleles (Fig. 1a), in which viral enhancers activate an endogenous promoter that controls the transcription of an RNA lacking an annotated open reading frame[14] (see Supplementary Information). We initially described *jaw-D* mutants as having serrated leaves, but a more detailed inspection revealed that the primary defect is uneven leaf shape and curvature. Unlike those of wild type, *jaw-D* leaves cannot be flattened without cutting the margins, indicating that overall gaussian curvature is not zero (Fig. 1b). All of these abnormalities are reminiscent of those seen in snapdragon *cin* mutants[1]. Additional defects include cotyledon epinasty (Fig. 1b), a modest delay in flowering and crinkled fruits (Supplementary Information).

To understand the basis of the *jaw-D* phenotype, we analysed global expression profiles using duplicate Affymetrix arrays that represent over 24,000 annotated genes (NCBI-GEO series GSE518). Ranking by estimated reduction in expression level revealed that the top 40 genes included four *TCP* genes that are closely related to *CIN* from snapdragon. One other *TCP* gene with strong similarity to *CIN* was also downregulated (Fig. 1c), whereas the remaining *TCP* genes represented on the array showed no obvious changes. The effect of *jaw-D* on *TCP* expression was confirmed by reverse transcription followed by real-time polymerase chain reaction (Fig. 1c). The decreased expression of *CIN* homologues in *jaw-D* mutants readily explains the similar leaf phenotype of *jaw-D* and *cin* mutants.

Alignment of the *TCP* genes whose expression was reduced in *jaw-D* mutants revealed a conserved, seven-amino-acid motif outside the TCP domain that was missing in the *TCP* genes unaffected by *jaw-D* (Supplementary Information). The RNA sequence encoding this motif is almost invariant and has few synonymous substitutions. This RNA motif is not restricted to *CIN* homologues, and a

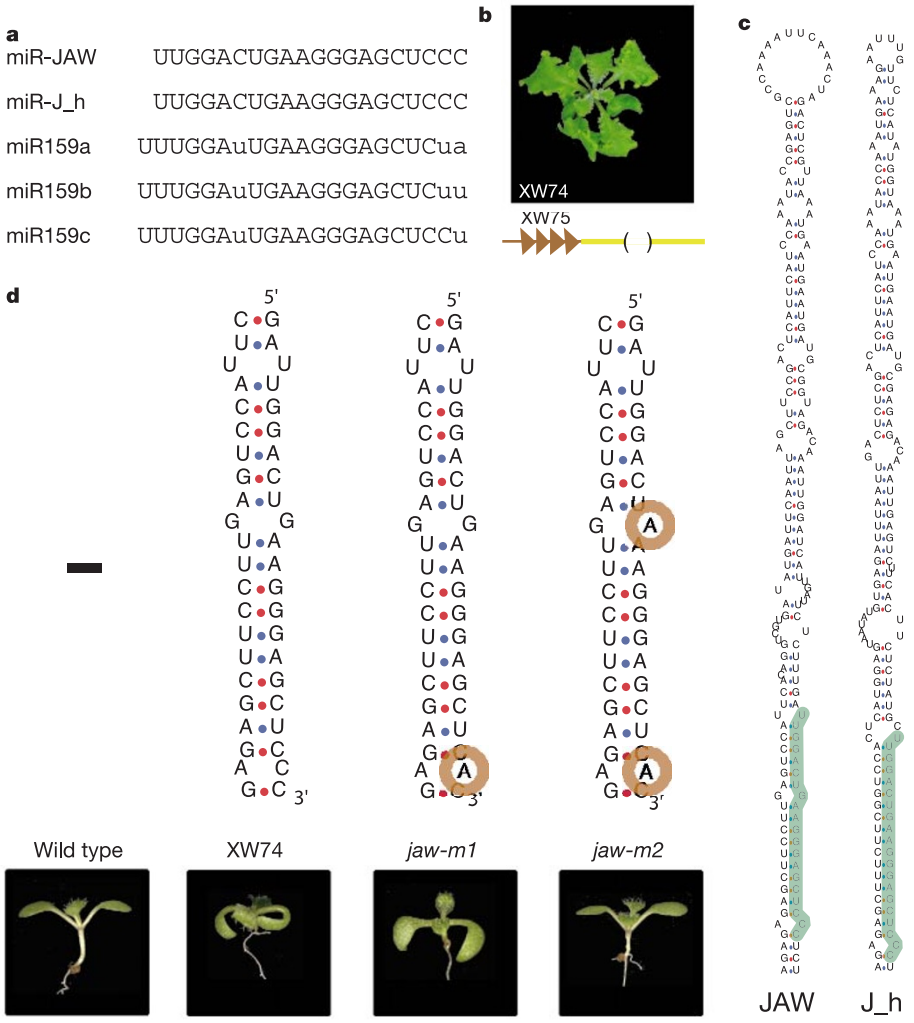

Figure 2 *JAW* encodes a microRNA. **a**, Sequence similarity of predicted miRNA from the *JAW* locus and its homologue (miR-J_h) with miR159 isoforms. **b**, The *jaw-D* phenotype was recapitulated in 106 of 151 wild-type plants transformed with pXW74, which contains a 1.4-kb fragment with adjacent *35S* enhancers isolated from *jaw-3D* (see Fig. 1a). pXW75 has a 226-bp deletion and does not cause the *jaw-D* phenotype (108 transformants). **c**, Predicted fold-back structures of the miRNA precursors of *JAW* and its homologue (J_h) from BAC MBK23. The green lines at the right indicate the miRNAs. **d**, Effect of *JAW* point mutations in transgenic seedlings (in the context of pXW74). *jaw-m1* causes slight epinasty of cotyledons, but does not affect rosette or cauline leaves. *jaw-m2* lacks dominant *JAW* activity.

related sequence is also found in several *MYB* genes (see below). Furthermore, this motif was partially complementary to miR159 (refs 7, 9), and to a sequence at the *JAW* locus (Fig. 2a).

A miRNA encoded by *JAW*

To test the function of the motif conserved between *TCP* genes and *JAW*, we introduced a 226-base pair (bp) deletion in a genomic fragment that, when linked to *35S* viral enhancers, recapitulated the *jaw-D* phenotype in transgenic plants (Figs 1a and 2b). The deleted version had lost all *JAW* activity. The deletion region can potentially give rise to an extended fold-back structure reminiscent of miRNA precursors, and a similar structure may form from a second *Arabidopsis* locus (Fig. 2c). The motif that is partially complementary to the *TCP* mRNAs, and which begins with a U like the majority of plant miRNAs[7,9,12], is located at the base of the putative stems. Two point mutations, in the middle and near the end of the conserved motif, were introduced into the *jaw-D* genomic fragment. Quantitative polymerase chain reaction with reverse transcription (RT–qPCR) of transgenic plants showed that production of the *JAW* RNA was not affected by these mutations (Supplementary Information). A fragment containing only the substitution at the terminal conserved position lacked most of the *JAW* activity, whereas the double mutation eliminated *JAW* activity (Fig. 2d).

We hybridized a low-molecular mass RNA blot with a 20-nucleotide probe complementary to the predicted miRNA encoded by *JAW*. This probe detected an RNA from inflorescences that co-migrated with a synthetic 20-nucleotide RNA starting with a U (Fig. 3a). It hybridized much more weakly to a larger species that co-migrated with a 21-nucleotide standard. Most miRNAs accumulate to elevated levels in plants expressing the RNA silencing suppressor P1/HC-Pro from potyviruses[12,13,15]. This was also the case for the 20- and 21-nucleotide RNA detected by the *JAW* probe. Conversely, as with other miRNAs[7,9,12], these RNAs were decreased in a *dcl1* mutant. In *jaw-D*, predominantly the level of the 20-nucleotide species was increased. A probe for the related miRNA miR159 detected preferentially a 21-nucleotide species with little change in *jaw-D* (Fig. 3a). Together, these data are consistent with *JAW* encoding a 20-nucleotide miRNA, miR-JAW, which is distinct from the 21-nucleotide miR159. The 21-nucleotide species detected by the *JAW* probe may reflect the presence of a minor, modified form of miR-JAW, or cross-hybridization to miR159.

Using RT–qPCR, we found that the *MIR-JAW* precursor was more abundant in the shoot apex, inflorescence and siliques, and elevated in *jaw-D* mutants (Fig. 3b), mimicking the differential accumulation of the processed miRNA in different tissues and in *jaw-D*.

As plant miRNAs have been shown to guide target RNA cleavage[3,4,12], we determined whether *TCP* mRNAs were at least partially cleaved in wild-type plants. Cleavage products of all five *TCP* genes were detected using a previously described rapid amplification of cDNA ends (RACE) procedure[12] (Fig. 4a). The predominant cleavage site in each mRNA was opposite position 10 from the 5′ end of miR-JAW (Fig. 4a)—which is a hallmark of miRNA- and siRNA-guided cleavage[12,16]—thus confirming the assignment of the miR-JAW sequence. Although their low levels made detection by RNA blot difficult, fragmentation products of *TCP2* and *TCP4* appeared to be increased in *jaw-D* mutants relative to wild type (Fig. 4b). The probe sets on the Affymetrix arrays detect both full-length transcripts and 3′ cleavage fragments, whereas the RT–qPCR products correspond only to uncleaved transcripts (Fig. 1a). This may explain differences in the magnitude of expression changes estimated from Affymetrix and RT–qPCR experiments.

As described above, miR-JAW also shows partial sequence complementarity to several *MYB* genes, which were predicted to be miR159 targets[9,17]. Specific cleavage sites were detected in *MYB33* and *MYB65* mRNAs (Fig. 4a), but not in *MYB104* (not shown). The cleavage sites are opposite position 10 from the 5′ end of miR159, but only nine nucleotides downstream from the 5′ end of miR-JAW. Consistent with the *MYB* genes being primarily targeted by miR159 or other, not yet identified miRNAs, the three genes were unaffected in *jaw-D* plants as determined by microarray analysis (NCBI-GEO series GSE518).

In vivo role of miRNA-guided degradation

If cleavage of *TCP* mRNAs guided by miRNAs has a role *in vivo*, we expect *TCP* RNAs to be expressed in specific patterns. RT–qPCR showed that levels of *TCP2* and *TCP4* RNA vary between different tissues. We chose to analyse *TCP4* in more detail by *in situ* hybridization because its expression was strongly affected in *jaw-D* mutants. The dynamic pattern of *TCP4* expression during embryogenesis and leaf development (Fig. 5) is consistent with *TCP4* having an instructive role in regulating the growth of cotyledons and leaves, both of which are affected in *jaw-D* mutants.

To determine the importance of miRNA-guided cleavage of *TCP4* mRNA, we engineered miRNA-resistant versions of *TCP4*. We first tested the effects of synonymous substitutions that changed the miR-JAW target sequence, but not the encoded amino acid sequence, in reconstruction experiments[3] (Fig. 4a, c). In these experiments, two types of *Agrobacterium* strains were co-injected

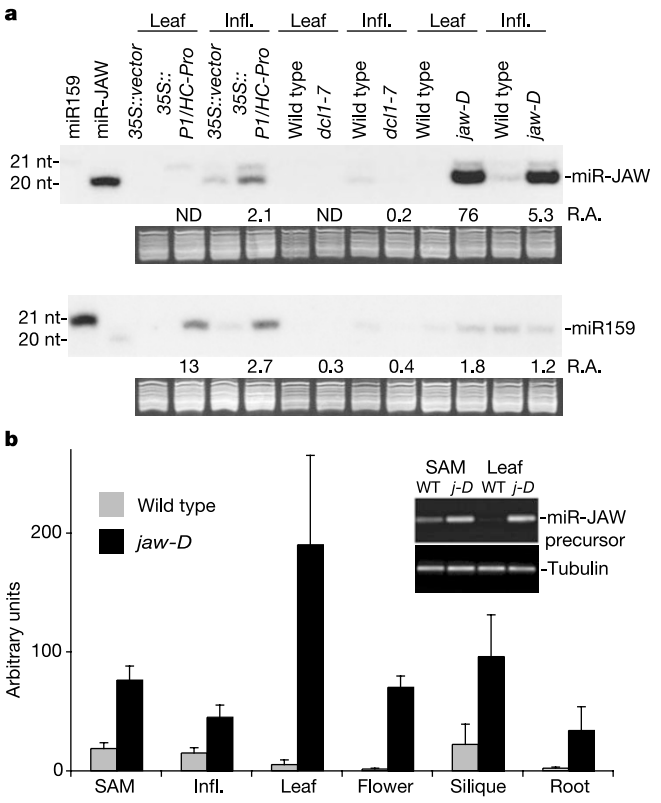

Figure 3 miR-JAW and miR159 expression. **a**, Blots of low-molecular-mass RNA extracted from leaves or inflorescences (Infl.) of different genetic backgrounds, next to synthetic miR159 (21 nucleotides) and miR-JAW (20 nucleotides). Note that there is minor cross-hybridization of the miR-JAW probe (top) and the miR159 probe (bottom). 35S::vector, empty vector control; 35S::P1/HC-Pro, *35S* promoter driving expression of P1/HC-Pro. *dcl1-7* and *jaw-1D* are in different wild-type backgrounds, and different controls were used accordingly. Relative accumulation (R.A.) of miRNAs compared with the respective wild-type controls is indicated. Ethidium bromide-stained gels are shown as loading control. **b**, Expression of *MIR-JAW* precursor in different tissues of wild-type and *jaw-1D* relative to tubulin, monitored by RT–qPCR. Each bar represents the average of at least three independent samples. The inset shows examples of amplification products from shoot apical meristem (SAM) and leaf tissues separated on an agarose gel.

into a heterologous host, *Nicotiana benthamiana*. The first strain contained a construct in which either *TCP4* or a mutant derivative, *mTCP4*, was under the control of the constitutive *35S* promoter. The second strain contained either an empty vector or *35S::JAW*. The full-length *35S::TCP4* transcripts were destabilized by co-injection of *35S::JAW*, resulting in accumulation of cleavage products. In contrast, *35S::JAW* had no effect on *35S::mTCP4* transcript stability (Fig. 4c), demonstrating that the synonymous mutations in *mTCP4* strongly decrease susceptibility to miRNA-guided cleavage.

Next, we introduced the same mutations in the genomic context of the *TCP4* gene. Most (35 of 57) primary transformants carrying the mutated version of *TCP4* were arrested at the seedling stage (Fig. 6a), with a range of phenotypes reminiscent of embryonic patterning mutants such as *monopteros* or *cup-shaped cotyledons*[18,19]. Common defects included fusion of the cotyledons, lack of a shoot apical meristem and overall tubular shape of the seedlings, resembling the effects of auxin inhibitors on wild-type embryos[20]. Surviving transformants had a range of defects, including bushy rosettes and abnormal inflorescences. None of 80 primary transformants containing a wild-type construct showed such defects. Together, these observations indicate that miRNA-mediated control of *TCP4* expression is essential for plant development.

Control of *TCP* mRNA abundance by miRNAs

If miRNA-guided cleavage is the major control point for regulating abundance and distribution of *TCP* genes, constitutive expression of their mRNAs should have few phenotypic effects, as long as they are susceptible to degradation. To test this hypothesis, we compared the effects of overexpressing wild-type RNAs with the effects of overexpressing RNAs with altered miRNA target sequences (Fig. 4a).

35S::TCP2 plants had no obvious defects (100 primary transformants examined). RNA blots showed that transcripts from the *35S::TCP2* transgene accumulated to much lower levels than transcripts from the *35S::mTCP2* transgene (Fig. 4b), which had similar synonymous mutations to *mTCP4* (Fig. 4a). The increases in *TCP2* full-length transcripts, as detected by RT–qPCR and RNA blots, were at most twofold (Fig. 4b; see also Supplementary Information). In contrast to the wild-type construct, marked phenotypic

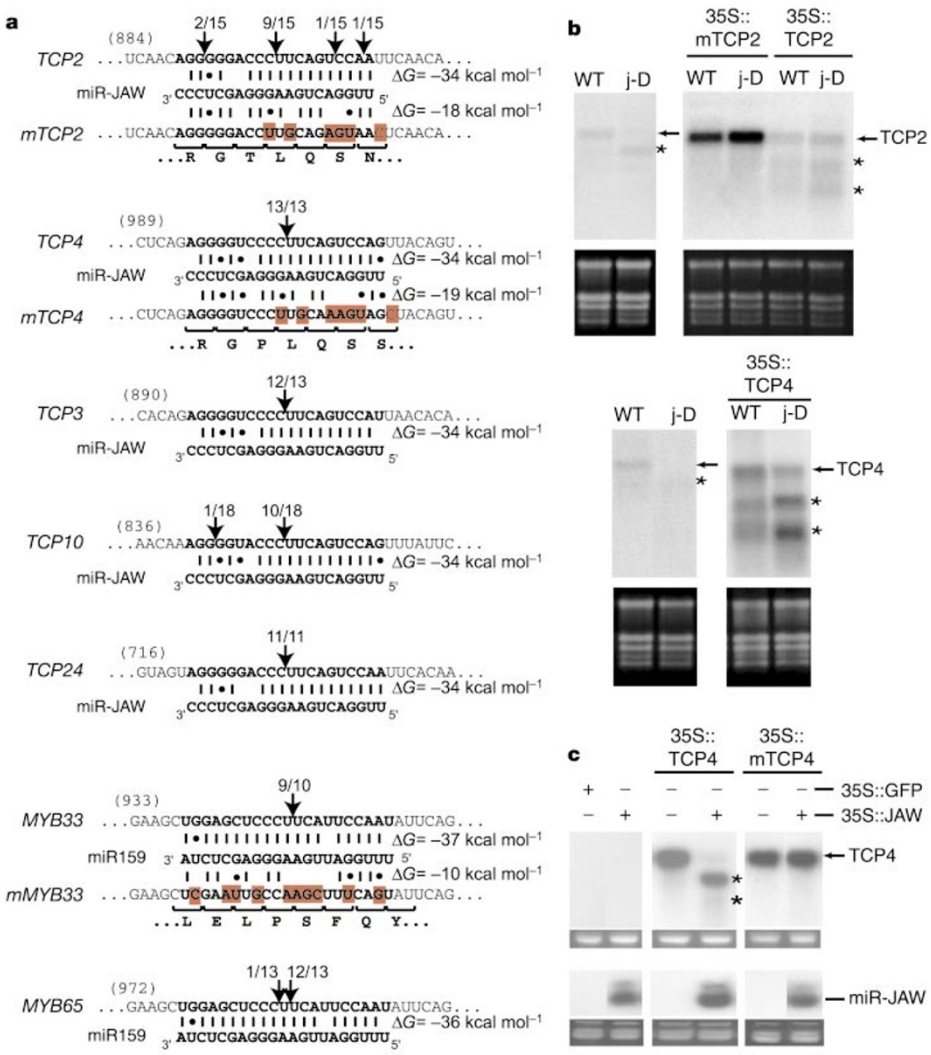

Figure 4 Identification of miRNA-guided cleavage products. **a**, Mapping of cleavage sites by 5′ RACE-PCR[12]. Partial mRNA sequences from five *TCP* and two *MYB* genes were aligned with miR-JAW and miR159, respectively. Free energies of duplex structures as calculated using mfold[39] are indicated on the right. Numbers indicate the fraction of cloned PCR products terminating at different positions. Shaded positions indicate synonymous changes introduced into miRNA target sites. **b**, Blots of high-molecular-mass RNA from different *Arabidopsis* lines. Arrows indicate intact mRNA molecules; asterisks indicate fragments resulting from miRNA-guided cleavage. The ratio of full-length transcripts to cleavage products was always lower in *jaw-1D*. **c**, Blots of high-molecular-mass (top) and low-molecular-mass (bottom) RNA from *N. benthamiana* leaves co-infiltrated with different *Agrobacterium* strains. The 20-nucleotide RNA corresponding to miR-JAW was detected only in leaves injected with *35S::JAW* (pXW74). A less prominent 21-nucleotide species was also detected. Ethidium bromide-stained gels are shown as loading controls.

effects were frequent with *35S::mTCP2*, consistent with the substantially higher levels of full-length transcripts (Fig. 4b; see also Supplementary Information). Many (30 of 71) *35S::mTCP2* plants had longer hypocotyls than wild type, they were smaller and greener, and their apical dominance was reduced (Fig. 6b).

A similar picture was seen with *TCP4*. Most (63 of 76) primary *35S::TCP4* transformants were phenotypically normal, with the remainder having slightly longer hypocotyls and smaller leaves than wild type (not shown). In contrast, most (55 of 68 of primary transformants) of the *35S::mTCP4* plants had marked pattern defects (Fig. 6c), similar to plants with the mutant *TCP4* form under control of the endogenous promoter, but at a slightly higher frequency (81% compared with 61% of transformants).

From experiments with mutated *MYB33* we conclude that miRNA regulation of *MYB33* is important as well. Whereas *35S::MYB33* had no obvious effect on development, *35S::mMYB33* caused leaves to curl upwards in many (39 of 63) primary transformants (Fig. 6d).

TCP mRNA degradation causes *jaw-D* phenotypes

To confirm that degradation of target mRNAs was indeed the cause for *jaw-D* phenotypes, we introduced constructs expressing wild-type and miRNA-resistant forms of target genes into *jaw-D* mutants. Constitutive expression of wild-type *TCP2* or *TCP4* partially rescued the leaf defects of *jaw-D* mutants. Leaves were less warped and elliptical than those of the parental line, but were still distinct from those of wild type (Fig. 6e). The suppression of the *jaw-D* phenotype was paralleled by an increase in *TCP2* or *TCP4* full-length RNA (Fig. 4b). RT–qPCR confirmed that rescue was not due to co-suppression and thereby reduced expression of the *MIR-JAW* precursor (Supplementary Information).

The mutant version of *TCP2* was able to rescue the leaf shape and curvature defects of *jaw-D* more extensively than *35S::TCP2* (Fig. 6d). The level of full-length *mTCP2* mRNA from the transgene was similar in wild-type and *jaw-D* backgrounds, and substantially higher than either the endogenous mRNA or the *TCP2* mRNA produced from the non-mutated *35S::TCP2* construct (Fig. 4b). The correlation between rescue and amount of full-length transcripts was further confirmed by RT–qPCR (Supplementary Information). The *35S::mTCP4* construct caused the same severe defects in *jaw-D* as in a wild-type background (not shown). Because these plants did not produce clearly identifiable cotyledons or leaves, rescue of the *jaw-D* phenotype could not be assessed. Expression of *mTCP4* from the *TCP4* promoter had less extreme effects than *35S::mTCP4* (see above), and the *jaw-D* leaf phenotype was suppressed in 11 of 15 surviving primary transformants. Notably, these plants showed a new phenotype: rounder leaves (Supplementary Information).

Constitutive expression of mutated *MYB33* in *jaw-D* mutants caused an additive phenotype (not shown), consistent with the observation that *MYB33* RNA was not reduced in *jaw-D* mutants, and further supporting the suggestion that *MYB33* is primarily targeted by an miRNA other than miR-JAW, probably miR159.

MIR-JAW and miRNA target-site selection

Expressed sequence tags (ESTs) with similarity to the *MIR-JAW* precursor were found in several species, including wheat and soybean (Supplementary Information). All ESTs are much longer than the predicted fold-back structure in *MIR-JAW*, similar to the approximately 500-base *JAW* transcript from *Arabidopsis*[14], suggesting that sequences flanking the fold-back structure are important for miRNA processing, even though there is little similarity at the primary sequence level.

Database searches also identified homologues of candidate miR-JAW targets among *TCP* genes in several species. All 11 proteins encoded by genes containing an miRNA target site belong to a monophyletic clade within the class II TCP subgroup (Fig. 1c), indicating that the miRNA target sequence arose only once among the *TCP* genes.

When we compared divergence of coding sequences for TCP domains and miRNA target motifs, we found similarly low rates of non-synonymous changes ($K_A = 0.17$ and 0.12, respectively), but a much higher rate of synonymous changes ($K_S = 1.22$) in the TCP domain than in the miRNA target motif ($K_S = 0.35$), indicating that the selective forces acting on the miRNA target motif are different from those that shape the TCP domain (see Supplementary Information for details).

Discussion

MicroRNAs and siRNAs, which have been found in all complex eukaryotes examined, regulate the activity of target genes through at least two distinct mechanisms. In both plants and animals, siRNAs with perfect complementarity trigger degradation of their target mRNAs[4,21,22]. In contrast, the predominant mode of miRNA action in animals seems to be translational control, as originally shown for the prototypical miRNAs produced by the *let-7* and *lin-4* genes of *Caenorhabditis elegans*[23–25], and more recently for *bantam* in *Dro-*

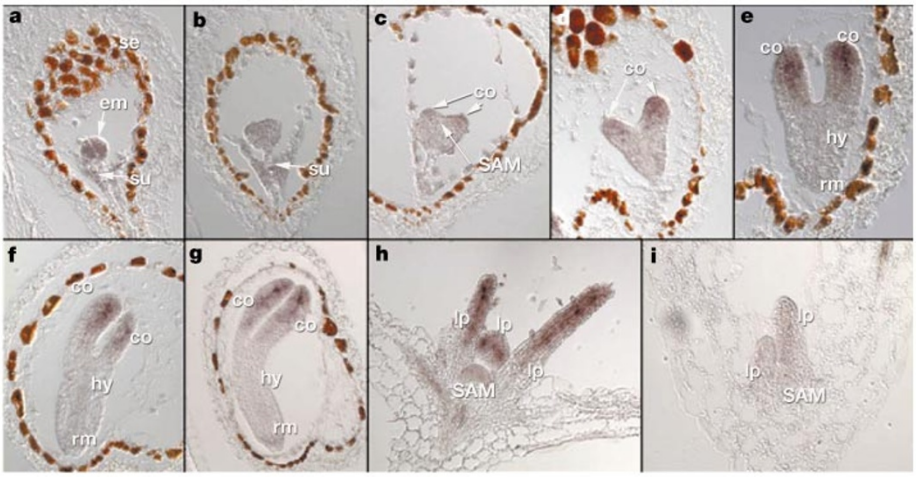

Figure 5 Expression pattern of *TCP4* mRNA. **a**–**g**, *In situ* localization of *TCP4* mRNA in wild-type embryos of progressive age. From an initially uniform pattern during the globular stage (**a**), *TCP4* RNA becomes gradually restricted to emerging cotyledons during the heart stage (**d**). During the torpedo stage, *TCP4* RNA becomes localized to subepidermal regions of the cotyledons, with highest levels near the tip (**e**–**g**). **h**, A similar pattern as in cotyledons is seen in young leaves of a wild-type seedling. **i**, *TCP4* RNA signal is reduced in *jaw-D* seedlings. co, cotyledon; em, embryo proper; hy, hypocotyl; lp, leaf primordium; rm, root meristem; SAM, shoot apical meristem; se, seed coat; su, suspensor.

sophila melanogaster[26] and miR-23 in human cells[27]. Although naturally occurring animal miRNAs are able to target artificial, perfectly complementary mRNAs for destruction[28], their normal targets have only limited complementarity, which apparently prevents degradation of the target RNAs.

In plants, it is unknown whether miRNAs are involved in translational control, but there are several examples of mRNAs that are cleaved in positions complementary to endogenous miRNAs[3,4,12,13]. Circumstantial evidence for this mechanism being important in regulating accumulation of specific mRNAs came initially from an analysis of dominant mutations at the *PHV* locus. These mutations affect RNA cleavage in a cell-free system[4] and cause aberrant accumulation of *PHV* mRNA *in vivo*[29]; however, because they also change the amino acid sequence of a potential regulatory motif predicted to be involved in sterol- or lipid-binding, it was unclear whether the primary defect is indeed in aberrant mRNA accumulation, and not, as originally proposed[29], due to a change in protein function.

We identified a new miRNA, miR-JAW, using a genetic screen, along with a new set of miRNA targets related to the *CIN* gene[1] of snapdragon. These targets constitute a subset of *TCP* genes, which, in contrast to several other transcription factor genes with potential roles in development, had not been previously recognized as candidate miRNA targets. We have shown that miRNA-directed cleavage of *TCP* mRNAs is not only required for normal development, but that it is also the main control point for regulating mRNA accumulation.

CIN mRNA is normally downregulated in non-dividing, differentiating cells. Developing leaves of *cin* mutants therefore suffer from a delay in cell division arrest (and subsequent differentiation), leading to accumulation of excess cells at the periphery and a crinkled leaf phenotype[1]. Thus, miRNA-mediated control of *CIN* and other target *TCP* genes is probably required for proper timing of the transition between cell division and differentiation in developing leaves. Both the *MIR-JAW* precursor and the miRNA target motif in *TCP* genes are found across a wide range of flowering plants, even though these have very different leaf morphologies and modes of leaf development. This observation supports a conserved role of the *CIN*-class of *TCP* genes in controlling leaf morphogenesis.

Although the growth-arrest phenotype of dominant *TCP4* mutants is consistent with a role of *Arabidopsis TCP* genes in differentiation, some of the dominant *TCP2* phenotypes, such as elongated hypocotyls or reduced apical dominance, are not readily explained by growth inhibition. Conversely, *jaw-D* mutants have phenotypes in addition to crinkly leaves, such as late flowering, suggesting additional roles for *TCP* genes and miR-JAW targets. A further layer of complexity is added by the fact that the *Arabidopsis* genome contains at least two regions with the potential to produce miR-JAW, as well as several potential precursors for a family of three almost identical miRNAs (miR159a–c) that are related to miR-JAW. In contrast to miR-JAW, miR159 is predicted to preferentially target three *MYB* genes, as miR159 shows better complementarity with the *MYB* than the *TCP* genes.

Our finding that only overexpression of an miRNA-resistant form of *MYB33* has major phenotypic consequences provides strong evidence for miRNA regulation of *MYB33*. It does not discriminate between miRNA-controlled RNA cleavage and translational repression, which leaves several possible explanations for the absence of an effect of *jaw-D* on *MYB* RNA expression. Our favourite model is that *MYB* genes are not cleaved by miR-JAW, but by other miRNAs such as miR159. Alternatively, translational regulation of *MYB* genes by miRNAs may be more important than mRNA cleavage. These observations highlight the importance of examining predicted targeting events *in vivo*.

The complex relationships between related miRNAs on the one hand and overlapping sets of potential targets on the other hand indicates that the miRNA regulatory network is similarly intricate compared with transcriptional networks in which families of related DNA-binding proteins control overlapping sets of target genes. Global transcript analysis, together with miRNA overexpression and the engineering of miRNA-resistant target genes, as implemented in our study, should be powerful tools for dissecting the miRNA regulatory network in plants.

Note added in proof: Overexpression experiments suggest that some plant miRNAs act also through translational control[40]. □

Figure 6 Effects of miRNA-resistant transgenes and *trans*-complementation of *jaw-1D*. **a**, Different patterning defects in seedlings transformed with a genomic copy of *TCP4* containing point mutations in the miRNA target site (see Fig. 4a). **b**, Plants that overexpress mutated *TCP2* (*35S::mTCP2*); note the elongated hypocotyls shown in the inset (wild type to the left). **c**, Patterning defects in *35S::mTCP4* seedlings; compare to **a**. **d**, Effects of mutated *MYB33* (*35S::mMYB33*) on rosette morphology. **e**, Partial to complete complementation of the *jaw-D* leaf phenotype by overexpressing wild-type *TCP2* and *TCP4*, or mutated *TCP2*.

Methods

Plant material

Plants were grown in long days (16 h light/8 h dark) under fluorescent lights at 23 °C. *jaw-1D*, *jaw-2D*, *dcl1-7* and *35S::P1/HC-Pro* plants have been described[10,12,14]. *jaw-3D* and *jaw-4D* were isolated using pSKI015 (ref. 14). Transgenic plants were generated as described[30].

Transgenes

The genomic fragment used in pXW74 was obtained by plasmid rescue[14]. *TCP* and *MYB* complementary DNAs were amplified from a Columbia cDNA library (gift of P. Wigge). Mutated versions of *TCP*genes and *MYB33* were generated by PCR. Promoter sequences of *TCP4* were isolated from genomic DNA by PCR. All amplification products were verified by sequencing. Primer sequences are available on request.

Microarray analysis

RNA was extracted using the Plant RNeasy Mini kit (Qiagen). Double-stranded cDNA was synthesized from 10 μg total RNA using the Superscript Choice System (Invitrogen) and

an oligonucleotide dT-T7 primer (Genset). cDNA was converted to biotinylated cRNA using the BioArray High Yield Transcript Labelling kit (Enzo). cRNA was cleaned with RNeasy columns (Qiagen) according to the manufacturer's protocol, with the following modifications. First, the cRNA was passed through the column twice to increase binding. Second, the eluate was re-applied to the column once to increase yield. Usually, 50–100 μg cRNA were obtained. Twenty micrograms of concentration-adjusted cRNA were fragmented and hybridized to GeneChip arrays according to the manufacturer's protocol (Affymetrix). For washing and staining, protocol EukGE-WSv4 was used. Expression values were estimated using Microarray Suite v5.0 (Affymetrix) or robust multi-array analysis[31].

Real-time RT–PCR

Reverse transcription was performed with 1 μg total RNA, using a kit (Promega). PCR was carried out in the presence of the double-strand DNA-specific dye SYBR green (Molecular Probes). Amplification was monitored in real time with the Opticon Continuous Fluorescence Detection System (MJR). Dual-labelled fluorogenic probes were used for TaqMan assays[32]. Primer sequences are available on request.

Small RNA isolation and blot analysis

Total RNA was isolated from fully expanded leaves and inflorescence clusters (containing stage 1–12 flowers; ref. 33) using Trizol reagent (Invitrogen). Low-molecular-mass RNA was separated from high-molecular-mass RNA using Qiagen Midi preps, and resolved by 17% PAGE under denaturing conditions[3]. A total of 250 pg synthetic RNA oligonucleotides that were 5′ phosphorylated (Dharmacon Research) were included as size standards. Blots were hybridized using end-labelled oligonucleotide probes[3]. Hybridization signal was measured using an InstantImager (PerkinElmer).

Cleavage site mapping of miRNA targets

An RNA ligase-mediated 5′ RACE procedure was used to map the cleavage site of miRNA targets as described[12]. Total RNA from 4-week-old *Arabidopsis* (Col-0) leaves and inflorescences was used for poly(A)$^+$ mRNA preparation. After amplification, 5′ RACE products were gel-purified and cloned, and at least ten independent clones were sequenced. Primer sequences are available on request.

In situ hybridization

Previously published methods[30] were used with modifications, including the use of an automated embedding system (Leica).

Phylogenetic analysis

Sequences for full-length *TCP* genes were identified from GenBank by BLAST analysis. The gene names and their GenBank accession numbers are provided in Supplementary Information. Protein and *MIR-JAW* precursor sequences were aligned using Clustal[34]. *TCP* nucleotide sequences were aligned manually to match protein alignment. Phylograms were generated with PAUP* (ref. 35), using a heuristic search with Multrees option and the TBR swapping algorithm, using 100 replicates (bootstrap values shown in Fig. 1c). A total of 267 trees were generated by maximum parsimony. Bayesian analysis was performed using MrBayes[36], with the chains run for 2,000,000 generations. For nucleotide analysis, the third positions of codons were excluded. Synonymous and non-synonymous site changes between pairs of sequences were calculated using DnaSP[37]. A 21-nucleotide region encompassing the miRNA target sequence and corresponding 60-nucleotide regions from genes lacking the target motif were selected for analysis.

Received 21 June; accepted 31 July 2003; doi:10.1038/nature01958.
Published online 20 August 2003.

1. Nath, U., Crawford, B. C., Carpenter, R. & Coen, E. Genetic control of surface curvature. *Science* **299,** 1404–1407 (2003).
2. Cubas, P., Lauter, N., Doebley, J. & Coen, E. The TCP domain: a motif found in proteins regulating plant growth and development. *Plant J.* **18,** 215–222 (1999).
3. Llave, C., Xie, Z., Kasschau, K. D. & Carrington, J. C. Cleavage of *Scarecrow-like* mRNA targets directed by a class of *Arabidopsis* miRNA. *Science* **297,** 2053–2056 (2002).
4. Tang, G., Reinhart, B. J., Bartel, D. P. & Zamore, P. D. A biochemical framework for RNA silencing in plants. *Genes Dev.* **17,** 49–63 (2003).
5. Plasterk, R. H. RNA silencing: the genome's immune system. *Science* **296,** 1263–1265 (2002).
6. Hutvágner, G. *et al.* A cellular function for the RNA-interference enzyme Dicer in the maturation of the *let-7* small temporal RNA. *Science* **293,** 834–838 (2001).
7. Reinhart, B. J., Weinstein, E. G., Rhoades, M. W., Bartel, B. & Bartel, D. P. MicroRNAs in plants. *Genes Dev.* **16,** 1616–1626 (2002).
8. Carmell, M. A., Xuan, Z., Zhang, M. Q. & Hannon, G. J. The Argonaute family: tentacles that reach into RNAi, developmental control, stem cell maintenance, and tumorigenesis. *Genes Dev.* **16,** 2733–2742 (2002).
9. Park, W., Li, J., Song, R., Messing, J. & Chen, X. CARPEL FACTORY, a Dicer homolog, and HEN1, a novel protein, act in microRNA metabolism in *Arabidopsis thaliana*. *Curr. Biol.* **12,** 1484–1495 (2002).
10. Jacobsen, S. E., Running, M. P. & Meyerowitz, E. M. Disruption of an RNA helicase/RNAse III gene in *Arabidopsis* causes unregulated cell division in floral meristems. *Development* **126,** 5231–5243 (1999).
11. Golden, T. A. *et al. SHORT INTEGUMENTS1/SUSPENSOR1/CARPEL FACTORY*, a Dicer homolog, is a maternal effect gene required for embryo development in *Arabidopsis*. *Plant Physiol.* **130,** 808–822 (2002).
12. Kasschau, K. D. *et al.* P1/HC-Pro, a viral suppressor of RNA silencing, interferes with *Arabidopsis* development and miRNA function. *Dev. Cell* **4,** 205–217 (2003).
13. Xie, Z., Kasschau, K. D. & Carrington, J. C. Negative feedback regulation of *Dicer-Like1* in *Arabidopsis* by microRNA-guided mRNA degradation. *Curr. Biol.* **13,** 784–789 (2003).
14. Weigel, D. *et al.* Activation tagging in *Arabidopsis*. *Plant Physiol.* **122,** 1003–1013 (2000).
15. Mallory, A. C., Reinhart, B. J., Bartel, D., Vance, V. B. & Bowman, L. H. A viral suppressor of RNA silencing differentially regulates the accumulation of short interfering RNAs and micro-RNAs in tobacco. *Proc. Natl Acad. Sci. USA* **99,** 15228–15233 (2002).
16. Elbashir, S. M., Martinez, J., Patkaniowska, A., Lendeckel, W. & Tuschl, T. Functional anatomy of siRNAs for mediating efficient RNAi in *Drosophila melanogaster* embryo lysate. *EMBO J.* **20,** 6877–6888 (2001).
17. Rhoades, M. W. *et al.* Prediction of plant microRNA targets. *Cell* **110,** 513–520 (2002).
18. Mayer, U., Torres Ruiz, R. A., Berleth, T., Miséra, S. & Jürgens, G. Mutations affecting body organization in the *Arabidopsis* embryo. *Nature* **353,** 402–407 (1991).
19. Aida, M., Ishida, T., Fukaki, H., Fujisawa, H. & Tasaka, M. Genes involved in organ separation in *Arabidopsis*: an analysis of the *cup-shaped cotyledon* mutant. *Plant Cell* **9,** 841–857 (1997).
20. Hadfi, K., Speth, V. & Neuhaus, G. Auxin-induced developmental patterns in *Brassica juncea* embryos. *Development* **125,** 879–887 (1998).
21. Hamilton, A. J. & Baulcombe, D. C. A species of small antisense RNA in posttranscriptional gene silencing in plants. *Science* **286,** 950–952 (1999).
22. Hammond, S. M., Bernstein, E., Beach, D. & Hannon, G. J. An RNA-directed nuclease mediates post-transcriptional gene silencing in *Drosophila* cells. *Nature* **404,** 293–296 (2000).
23. Lee, R. C., Feinbaum, R. L. & Ambros, V. The *C. elegans* heterochronic gene *lin-4* encodes small RNAs with antisense complementarity to *lin-14*. *Cell* **75,** 843–854 (1993).
24. Wightman, B., Ha, I. & Ruvkun, G. Posttranscriptional regulation of the heterochronic gene *lin-14* by *lin-4* mediates temporal pattern formation in *C. elegans*. *Cell* **75,** 855–862 (1993).
25. Reinhart, B. J. *et al.* The 21-nucleotide *let-7* RNA regulates developmental timing in *Caenorhabditis elegans*. *Nature* **403,** 901–906 (2000).
26. Brennecke, J., Hipfner, D. R., Stark, A., Russell, R. B. & Cohen, S. M. *bantam* encodes a developmentally regulated microRNA that controls cell proliferation and regulates the proapoptotic gene *hid* in *Drosophila*. *Cell* **113,** 25–36 (2003).
27. Kawasaki, H. & Taira, K. Hes1 is a target of microRNA-23 during retinoic-acid-induced neuronal differentiation of NT2 cells. *Nature* **423,** 838–842 (2003).
28. Hutvágner, G. & Zamore, P. D. A microRNA in a multiple-turnover RNAi enzyme complex. *Science* **297,** 2056–2060 (2002).
29. McConnell, J. R. *et al.* Role of *PHABULOSA* and *PHAVOLUTA* in determining radial patterning in shoots. *Nature* **411,** 709–713 (2001).
30. Weigel, D. & Glazebrook, J. *Arabidopsis: A Laboratory Manual* (Cold Spring Harbor Laboratory Press, Cold Spring Harbor, New York, 2002).
31. Irizarry, R. A. *et al.* Summaries of Affymetrix GeneChip probe level data. *Nucleic Acids Res.* **31,** e15, doi:10.1093/nar/gng015 (2003).
32. Heid, C. A., Stevens, J., Livak, K. J. & Williams, P. M. Real time quantitative PCR. *Genome Res.* **6,** 986–994 (1996).
33. Smyth, D. R., Bowman, J. L. & Meyerowitz, E. M. Early flower development in *Arabidopsis*. *Plant Cell* **2,** 755–767 (1990).
34. Thompson, J. D., Gibson, T. J., Plewniak, F., Jeanmougin, F. & Higgins, D. G. The CLUSTAL-X windows interface: flexible strategies for multiple sequence alignment aided by quality analysis tools. *Nucleic Acids Res.* **25,** 4876–4882 (1997).
35. Swofford, D. L. PAUP: A computer program for phylogenetic inference using maximum parsimony. *Gen. Physiol.* **102,** 9A (1993).
36. Huelsenbeck, J. P. & Ronquist, F. MRBAYES: Bayesian inference of phylogenetic trees. *Bioinformatics* **17,** 754–755 (2001).
37. Rozas, J. & Rozas, R. DnaSP version 3: an integrated program for molecular population genetics and molecular evolution analysis. *Bioinformatics* **15,** 174–175 (1999).
38. Citerne, H. L., Luo, D., Pennington, R. T., Coen, E. & Cronk, Q. C. A phylogenomic investigation of *CYCLOIDEA-like TCP* genes in the Leguminosae. *Plant Physiol.* **131,** 1042–1053 (2003).
39. Zuker, M. Mfold web server for nucleic acid folding and hybridization prediction. *Nucleic Acids Res.* **31,** 3406–3415 (2003).
40. Chen, X. A microRNA as a translational repressor of APETALA2 in *Arabidopsis* flower development. *Science* published online 31 July 2003 (doi:10.1126/science.1088060).

Supplementary Information accompanies the paper on **www.nature.com/nature**.

Acknowledgements We thank I. Puga-Gonzalez for assistance and V. Ambros, S. Balasubramanian, J. Chory, M.-C. Kim, J. Lohmann, Y. Kobayashi and J. Spatafora for advice and discussion. This work was supported by fellowships from CONICET and Human Frontier Science Program Organization to J.F.P., from Life Sciences Research Foundation/US Department of Energy to X.W.; by grants from NSF and NIH to J.C.C. and NIH to D.W.; and by the Max Planck Society. D.W. is a Director of the Max Planck Institute.

Competing interests statement The authors declare that they have no competing financial interests.

Correspondence and requests for materials should be addressed to D.W. (weigel@weigelworld.org) or J.C.C. (carrington@orst.edu).